Mathematika 61 (2015) 457–474 © 2015 University College London
doi:10.1112/S0025579314000461

MOVING STONE IN THE HELE-SHAW FLOW

GENNADY MISHURIS, SERGEI ROGOSIN AND MICHAL WROBEL

Dedicated to Professor V. Maz'ya on the occasion of his 75th birthday

Abstract. Asymptotic analysis of the Hele-Shaw flow with a small moving obstacle is performed. The method of solution utilizes the uniform asymptotic formulas for Green's and Neumann functions recently obtained by V. Maz'ya and A. Movchan. The theoretical results of the paper are illustrated by numerical simulations.

§1. *Introduction.* This paper is devoted to the asymptotic study of the flow in a Hele-Shaw cell in the presence of a moving obstacle in the flow.

The Hele-Shaw problem [14] deals with the description of the free boundary encircling the domain occupied by incompressible fluid in a so-called Hele-Shaw cell (see, for example, [12, 24]), i.e. in a narrow space between two parallel plates. Different driving mechanisms can be considered for the fluid flow, such as the presence of a source/sink in the fluid domain.

Various physical assumptions lead to different formulations of the respective boundary value problems. A comprehensive discussion on this topic can be found in the recent book by Gustafsson and Vasil'ev [12].

There exist two basic mathematical models for the flow in the Hele-Shaw cell. The *complex-analytic model* is formulated as a nonlinear mixed boundary value problem with respect to a family of conformal mappings of the canonical domain onto the domain occupied by the fluid [22, 8]. See also [3] and references therein for a survey of recent results on the complex-analytic Hele-Shaw problem in doubly connected domains. We note that there are some similarities between the movement of the rigid body and the movement of bubbles in the flow (for a discussion of the latter process, see for example, the article [6] and references therein).

In our study we use the *real-variable model* proposed by Gustafsson [11] in which the flow is described by a family of parametrizations of the boundary of fluid domain (see also [15]). Among variants of the proof of existence and uniqueness for this model we mention the papers by Reissig [23] and by Escher and Simonett [7]. In its most general form, the proof of the existence and uniqueness of the classical solution and the regularity of the fluid boundary was given by Antontsev *et al* [1, 2].

The classical (real-variable) Hele-Shaw model can be reinterpreted as a mixed boundary value problem for the Laplace equation with respect to the unknown

Received 17 April 2014, published online 8 April 2015.
MSC (2010): 76D27, 35J25, 35R35 (primary).

https://doi.org/10.1112/S0025579314000461 Published online by Cambridge University Press

parametrization of the boundary and the corresponding Green function of this problem in the reference domain. When assuming the presence of a moving obstacle in the flow, we have to add an additional equation describing this movement. The aim of our work is to perform an asymptotic analysis for such a variant of the model and to construct an efficient and robust numerical routine to tackle the problem.

Application of asymptotic methods for the approximation of Green's function goes back to the classical paper by Hadamard [**13**]. Recently, Maz'ya and Movchan obtained a number of asymptotic formulas for Green's function related to different boundary value problems for a number of differential operators in the case of singular perturbations of the domains (see [**16**–**18**] and references therein).

Those results were used in [**19**] to model the Hele-Shaw flow with a fixed circular obstacle. To construct the computation scheme, we choose Green's formula with the Neumann condition on the external boundary of a doubly connected domain, and with a Dirichlet condition on its internal boundary. Then a preliminary transformation $\zeta = \varepsilon/z$ was made, leading to the creation of a system of differential equations for the original problem approximation. The existence of the reformulated Hele-Shaw problem follows immediately from the results of the paper [**7**].

The approximate system defined in this way was reduced to a system of first-order ordinary differential equations (ODEs), and tackled by a proposed numerical scheme. This approach proved its ability to solve the Hele-Shaw problem, providing sufficiently good accuracy of computations.

However, the scheme itself exhibited some disadvantages:

(1) in the case of a sink the lifetime of the approximate process was very short;
(2) in the case of a source we get numerical result only on a bounded interval of time.

The first difficulty could be expected from the theory of the Hele-Shaw problem, but the second one is a consequence of the instability of the numerical scheme. In the case of a moving obstacle this led to even worse results.

In this paper we consider the Hele-Shaw flow with a rigid inclusion moving in the direction of the flow without rotation. The friction between the limiting planes and the obstacle is accounted for. To avoid problems appearing in the case of the fixed obstacle, we use here the same Maz'ya–Movchan approach, but with a different uniform asymptotic formula for Green's function (without making any preliminary transformations, and thus interchanging the role of boundary conditions).

The paper is organized as follows. Section 2 describes the geometry of the problem and presents the (real-variable) Hele-Shaw model in a domain with a moving obstacle. The model is further reduced to the form containing an unknown parametrization of the boundary of the fluid domain, an unknown Green function of the corresponding mixed boundary value problem for the Laplace operator and unknown trajectory of the inclusion. Therefore we have to consider a system of equations consisting of the equation for the free boundary

https://doi.org/10.1112/S0025579314000461 Published online by Cambridge University Press

(the standard Hele-Shaw equation) and the equation of motion for the obstacle. In §3 we present the uniform asymptotic formula of Maz'ya and Movchan and describe its components. In §4 we determine the values of the components of the Maz'ya–Movchan formula corresponding to the model considered. The final form of the approximate system of differential equations is presented in §4.4. Finally, in §5 the aforementioned system is implemented in a numerical scheme which illustrates the results obtained. The numerical scheme to obtain the solution employs reduction of the system of governing equations to the system of ODEs of first order, where the velocity of the inclusion is introduced as an additional dependent variable. In order to solve the dynamic system we utilize the standard ODE solver from the Matlab package: ode45. The respective conformal mappings of the boundary curve are performed by means of the Schwartz–Christoffel toolbox. The derivatives of the mapping along the free boundary are computed by our own subroutines, based on the spline approximation. We show that the asymptotic expansion used for the Green function is effective and the computations based on that approach are stable and robust. An extended description of the numerics is given in [**20**].

§2. *Problem formulation.* Let us consider a slow fluid flow in a Hele-Shaw cell (i.e. in the narrow gap between parallel plates of distance h). The flow is induced by a source/sink (situated at the origin $O = (0, 0)$) of intensity Q. A fluid of viscosity μ occupies the bounded doubly connected domain $D_1(t)$ at the time instant $t \geqslant 0$ that takes the form $D_1(t) = D(t) \setminus F$, where $D(t)$ is a bounded simply connected domain, and the compact set $F \subset D(t)$ is a small obstacle embedded within the fluid. The obstacle is moving in the direction of flow without rotation and with friction coefficient κ (friction on the surfaces of the limiting plates). To avoid technical difficulties, we assume a circular shape of the obstacle of radius ε and center $\mathbf{z}_0(t)$ at each instant of time t.

Suppose that our initial geometry satisfies the following conditions†

$$\begin{gathered} c \leqslant \min \operatorname{dist}\{O, D(0)\} \leqslant \max \operatorname{dist}\{O, D(0)\} \leqslant 1, \\ \operatorname{dist}\{\partial F, \partial D(0)\} = d > \varepsilon, \quad d + 2\varepsilon > c. \end{gathered} \tag{2.1}$$

Following [**2**], the initial free boundary $\partial D(0)$ is to satisfy the smoothness assumptions

$$\partial D(0) \in \mathcal{C}^{2,\alpha}, \tag{2.2}$$

with certain fixed α, $0 < \alpha < 1$.

Omitting the standard description of the (real-variable) Hele-Shaw model (see, for example, [**12**, **15**]; cf. [**19**]) we arrive at the following problem with respect to the unknown parametrization $\mathbf{w}(s, t)$ of the free boundary $\Gamma(t) = \partial D(t)$ (i.e. the boundary value of the conformal mapping of the unit disc $\mathbb{U}$ onto the fluid domain $D_1(t)$), Green's function $\mathcal{G}(\mathbf{z}; \zeta; t)$ of the domain $D_1(t)$ and the center $\mathbf{z}_0(t)$ of the obstacle‡.

† Note that the constants c and d do not depend on δ.

‡ The unknown magnitudes $\mathbf{w}$, $\mathcal{G}$, $\mathbf{z}_0$ depend on time t from a right-sided neighborhood I of $t = 0$. In fact, for our problem we need to determine the value of $\mathcal{G}(\mathbf{z}; \zeta; t)$ only at the point $\zeta = O$, but we keep the extra variable ζ for computational reasons.

https://doi.org/10.1112/S0025579314000461 Published online by Cambridge University Press

Problem ($\mathrm{HS}_{\mathrm{move}}$). Find a triple $\{\mathbf{w}(s,t) = (w_1(s,t), w_2(s,t)); \mathcal{G}(\mathbf{z};\zeta;t); \mathbf{z}_0(t) = (z_{0,1}(t), z_{0,2}(t))\}$, satisfying the following conditions:

(i) $\mathbf{w}(s,t) \in \Gamma(t)$ for all $(s,t) \in \partial\,\mathbb{U} \times I$;
(ii) $\mathbf{w}(\cdot,t) : \partial\,\mathbb{U} \to \Gamma(t)$ is a $\mathcal{C}^2$-diffeomorphism for each fixed $t \in I$;
(iii) $\mathbf{w}^{(0)}(s) = \mathbf{w}(s,0)$ is a given $\mathcal{C}^2$-diffeomorphism of the unit circle $\partial\,\mathbb{U}$, which describes the boundary $\Gamma(0)$ of initial domain $D_1(0)$;
(iv) $\mathcal{G}(\mathbf{z};\zeta;t)$ is Green's function of the operator $-\triangle$ in the doubly connected domain $D_1(t)$ with the homogeneous Neumann condition on ∂F and the homogeneous Dirichlet condition on $\Gamma(t)$;
(v) $\partial_t\,\mathbf{w}(s,t) = -(Qh^2/12\mu) \cdot \nabla\mathcal{G}(\mathbf{w}(s,t); O; t)$ for all $(s,t) \in \partial\,\mathbb{U} \times I$;
(vi) $\mathbf{z}_0'' + (\kappa\pi\delta^2/m)\mathbf{z}_0' = (Q\delta/m)\int_0^{2\pi} \mathcal{G}(z_{0,1} + \delta\cos\theta, z_{0,2} + \delta\sin\theta; O; t) \cdot \mathbf{n}^{(\mathrm{in})}(\theta)\,d\theta$,
(vii) $\mathbf{z}_0(0) = \mathbf{z}^{(0)}$, $\mathbf{z}_0'(0) = \mathbf{z}^{(1)}$.

The aim of our study is to get an approximate solution to Problem ($\mathrm{HS}_{\mathrm{move}}$).

§3. *Uniform representation of Green's function.* In order to replace the system of equations (i)–(vii) of Problem ($\mathrm{HS}_{\mathrm{move}}$) by the approximate system we use one of the results by Maz'ya and Movchan. It will be convenient to introduce here a small parameter ε equal to the radius of the inclusion, and denote by $F_0 = F_0(t)$ the rescaled obstacle $F_0(t) = \{\mathbf{x} : (1/\varepsilon)(\mathbf{x} - \mathbf{z}_0(t)) \in F\}$. Note that for each $t \in I$ we have $F_0(t) = B(O;1)$.

For the reader's convenience, we reformulate in our notation the theorem by Maz'ya and Movchan providing a uniform asymptotic approximation of Green's function with the Neumann data on the boundary of the obstacle $F = B(\mathbf{z}_0, \varepsilon)$ and the Dirichlet data on the boundary of the domain D.

THEOREM 3.1 [**18**, Theorem 2.1]. *Let D_1 be a bounded doubly connected domain in $\mathbb{R}^2$ with a smooth boundary, $D_1 = D\backslash F$, where D is a simply connected domain and $F \subset D$ is a compact set (obstacle) with diameter smaller than the distance from ∂F to ∂D.*

Green's function $\mathcal{G}_\varepsilon(\mathbf{x},\mathbf{y})$ of the Laplace operator $-\Delta$ with the Neumann zero data on ∂F and the Dirichlet zero data on ∂D has the following uniform asymptotic representation:

$$\begin{aligned}\mathcal{G}_\varepsilon(\mathbf{x},\mathbf{y}) = G(\mathbf{x},\mathbf{y}) + \mathcal{N}\left(\frac{1}{\varepsilon}(\mathbf{x}-\mathbf{z}_0), \frac{1}{\varepsilon}(\mathbf{y}-\mathbf{z}_0)\right) + \frac{1}{2\pi}\log\left|\frac{1}{\varepsilon}(\mathbf{x}-\mathbf{y})\right| \\ + \varepsilon\mathcal{D}\left(\frac{1}{\varepsilon}(\mathbf{x}-\mathbf{z}_0)\right) \cdot \nabla_{\mathbf{x}} H(\mathbf{z}_0,\mathbf{y}) \\ + \varepsilon\mathcal{D}\left(\frac{1}{\varepsilon}(\mathbf{y}-\mathbf{z}_0)\right) \cdot \nabla_{\mathbf{y}} H(\mathbf{x},\mathbf{z}_0) + \mathbf{r}_\varepsilon(\mathbf{x},\mathbf{y}), \qquad (3.1)\end{aligned}$$

where $|\mathbf{r}_\varepsilon(\mathbf{x},\mathbf{y})| \leqslant \mathrm{Const} \cdot \varepsilon^2$.

In what follows we use this formula in the fluid domain $D_1(t)$ for all $t \in I = [0,T]$, for which the solution to the Hele-Shaw problem exists and its boundary

https://doi.org/10.1112/S0025579314000461 Published online by Cambridge University Press

retains its initial smoothness. In the case of the flow without obstacle or with a fixed obstacle we refer for the existence, uniqueness and regularity results to [1]. In our case there is no rigorous proof of the existence, but it can be obtained similarly to that for the flow of bubbles (see, for example, [6] and references therein).

In our case we adopt in this theorem the following notation for each instant of time $t \in I$. $G(\mathbf{x}, \mathbf{y}) = G(\mathbf{x}, \mathbf{y}; t)$ is Green's function of the Laplace operator $-\Delta$ for the simply connected domain $D = D(t)$ with zero Dirichlet data on $\partial D(t)$:

$$G(\mathbf{x}, \mathbf{y}) = \frac{1}{2\pi} \log \left| \frac{1}{\mathbf{x} - \mathbf{y}} \right| - H(\mathbf{x}, \mathbf{y}), \tag{3.2}$$

with H being the regular part of Green's function, i.e. the harmonic function solving the following boundary value problem:

$$\Delta_{\mathbf{x}} H(\mathbf{x}, \mathbf{y}) = 0, \quad \mathbf{x}, \mathbf{y} \in D(t), \tag{3.3}$$

$$H(\mathbf{x}, \mathbf{y}) = \frac{1}{2\pi} \log \left| \frac{1}{\mathbf{x} - \mathbf{y}} \right|, \quad \mathbf{x} \in \partial D(t), \mathbf{y} \in D(t). \tag{3.4}$$

$\mathcal{N}(\xi, \eta)$ is the Neumann function for the exterior of the rescaled obstacle $F_0 = F_0(t)$:

$$\mathcal{N}(\xi, \eta) = \frac{1}{2\pi} \log |\xi - \eta|^{-1} - h_{\mathcal{N}}(\xi, \eta), \quad \xi, \eta \in \mathbb{R}^2 \backslash F_0(t), \tag{3.5}$$

where $h_{\mathcal{N}}(\xi, \eta)$ is the regular part of this function satisfying

$$\Delta_{\xi} h_{\mathcal{N}}(\xi, \eta) = 0, \quad \xi, \eta \in \mathbb{R}^2 \backslash F_0(t), \tag{3.6}$$

$$\frac{\partial h_{\mathcal{N}}(\xi, \eta)}{\partial n_{\xi}} = \frac{1}{2\pi} \frac{\partial}{\partial n_{\xi}} (\log |\xi - \eta|^{-1}), \quad \xi \in \partial F_0(t), \eta \in \mathbb{R}^2 \backslash F_0(t), \tag{3.7}$$

$$h_{\mathcal{N}}(\xi, \eta) \to 0, \quad |\xi| \to \infty, \eta \in \mathbb{R}^2 \backslash F_0(t). \tag{3.8}$$

The vector function $\mathcal{D}(\xi) = (\mathcal{D}_1(\xi), \mathcal{D}_2(\xi))^T$ is the solution of the following boundary value problems in the exterior of the rescaled obstacle $F_0 = F_0(t)$:

$$\Delta \mathcal{D}_j(\xi) = 0, \quad \xi \in \mathbb{R}^2 \backslash F_0(t), \ j = 1, 2, \tag{3.9}$$

$$\frac{\partial \mathcal{D}_j(\xi)}{\partial n} = n_j, \quad \xi \in \partial F_0(t), \ j = 1, 2, \tag{3.10}$$

$$\mathcal{D}_j(\xi) \to 0, \quad |\xi| \to \infty, \ j = 1, 2. \tag{3.11}$$

Here n_j are components of the inward unit vector normal to the boundary of disc $F_0(t)$.

https://doi.org/10.1112/S0025579314000461 Published online by Cambridge University Press

§4. *System of equations for Problem (HS_{move}).*

4.1. *Green's function $\mathcal{G}_\varepsilon$ for Problem (HS_{move}).* In this subsection we analyze the components of the representation (3.1). Let us first consider the Neumann function $\mathcal{N}(\xi,\eta)$ having in this case an explicit representation (see, for example, [**21**, p. 68]):

$$\mathcal{N}(\xi,\eta)=-\frac{1}{4\pi}\log|\xi-\eta|^2-\frac{1}{4\pi}\log\left[\frac{(|\xi|^2-1)(|\eta|^2-1)+|\xi-\eta|^2}{|\xi|^2|\eta|^2}\right] \tag{4.1}$$

satisfying conditions (3.5)–(3.8) and symmetric $\mathcal{N}(\xi,\eta)=\mathcal{N}(\eta,\xi)$. Its regular part $h_{\mathcal{N}}(\xi,\eta)$ is also symmetric, and explicit calculation yields

$$h_{\mathcal{N}}(\xi,\eta)=\frac{1}{4\pi}\log\left[\frac{(|\xi|^2-1)(|\eta|^2-1)+|\xi-\eta|^2}{|\xi|^2|\eta|^2}\right]. \tag{4.2}$$

Green's function $G(\mathbf{x};\mathbf{y};t)$ for the interior simply connected domain $D(t)$ can be represented in the form

$$G(\mathbf{x};\mathbf{y};t)=-\frac{1}{2\pi}\log|g(\mathbf{x},\mathbf{y})|, \tag{4.3}$$

where $g(\mathbf{x},\mathbf{y})=(g_1(\mathbf{x},\mathbf{y}),g_2(\mathbf{x},\mathbf{y})):D(t)\to\mathbb{U}$ is the conformal mapping of $D(t)$ onto the unit disc $\mathbb{U}$, satisfying the following normalizing conditions $g(\mathbf{x},\mathbf{y})|_{\mathbf{x}=\mathbf{y}}=0$, and $g'(\mathbf{x},\mathbf{y})|_{\mathbf{x}=\mathbf{y}}>0$. In our case, $\mathbf{y}=O$ stands for the source/sink point (we again note that from a computational point of view it is better to keep the extra variable $\mathbf{y}$ up to the final formula). From the numerical point of view it is customary to start with an arbitrary conformal mapping $g_0(\mathbf{x}):D(t)\to\mathbb{U}$ and determine the normalized one:

$$g(\mathbf{x},\mathbf{y})=\frac{g_0(\mathbf{x})-g_0(\mathbf{y})}{1-\overline{g_0(\mathbf{y})}g_0(\mathbf{x})}.$$

The vector function $\mathcal{D}(\xi)$ can be found by using an integral representation of the solution to the exterior Neumann problem for the unit disc (see, for example, [**21**, p. 68]). First we note that the inward unit normal vector on the boundary of the unit disc $F_0(t)$ is

$$\mathbf{n}^{(\mathrm{in})}=(n_1^{(\mathrm{in})},n_2^{(\mathrm{in})})=-(\cos\varphi,\sin\varphi), \tag{4.4}$$

where φ is the angular coordinate of the polar system on the unit circle $\partial F_0(t)$. Then the solutions to the problems (3.9)–(3.11) ($j=1,2$) are represented in the form

$$\mathcal{D}_j(\xi)=\frac{1}{2\pi}\int_0^{2\pi}\log\left(\frac{1}{r^2}+1-\frac{2}{r}\cos(\theta-\varphi)\right)n_j^{(\mathrm{in})}d\varphi,\quad j=1,2, \tag{4.5}$$

where $\xi=(r\cos\theta,r\sin\theta)$, $r>1$. It is easy to see that the above functions satisfy all conditions (3.9)–(3.11). We calculate (4.5) using [**10**, (4.397.6)]:

$$\mathcal{D}_1(\xi)=\frac{1}{2}\frac{\xi_1}{\xi_1^2+\xi_2^2},\qquad \mathcal{D}_2(\xi)=\frac{1}{2}\frac{\xi_2}{\xi_1^2+\xi_2^2}. \tag{4.6}$$

https://doi.org/10.1112/S0025579314000461 Published online by Cambridge University Press

4.2. *Derivatives of Green's function.* Here we calculate derivatives of Green's function which are used in equation (v) of Problem ($\mathrm{HS}_{\mathrm{move}}$). We start with Green's function $G(\mathbf{x};\mathbf{y}) = G(\mathbf{x};\mathbf{y};t)$. By applying representation (4.3) we have ($j = 1, 2$)

$$\partial_{x_j} G(\mathbf{x};\mathbf{y}) = -\frac{1}{2\pi}\frac{g_1(\mathbf{x};\mathbf{y})\partial_{x_j} g_1(\mathbf{x};\mathbf{y}) + g_2(\mathbf{x};\mathbf{y})\partial_{x_j} g_2(\mathbf{x};\mathbf{y})}{g_1^2(\mathbf{x};\mathbf{y}) + g_2^2(\mathbf{x};\mathbf{y})}. \tag{4.7}$$

Substituting $\mathbf{x} = (w_1(s,t), w_2(s,t))$, $\mathbf{y} = (0,0)$ and taking into account the properties of the function $g(\mathbf{x};\mathbf{y})$, we finally obtain

$$\begin{aligned}\partial_{x_j} G(w_1(s,t), w_2(s,t); 0, 0)\\ = -\frac{1}{2\pi}(g_1(w_1(s,t), w_2(s,t); 0, 0)\partial_{w_j} g_1(w_1(s,t), w_2(s,t); 0, 0)\\ + g_2(w_1(s,t), w_2(s,t); 0, 0)\partial_{w_j} g_2(w_1(s,t), w_2(s,t); 0, 0)).\end{aligned} \tag{4.8}$$

The Neumann function $\mathcal{N}(\xi;\eta)$ depends on the "scaled" variables

$$\xi = \frac{1}{\varepsilon}(\mathbf{x} - \mathbf{z}_0(t)), \qquad \eta = \frac{1}{\varepsilon}(\mathbf{y} - \mathbf{z}_0(t)). \tag{4.9}$$

Hence

$$\partial_{x_j}\mathcal{N}(\xi;\eta) = \partial_{\xi_j}\mathcal{N}(\xi;\eta)\frac{\partial \xi_j}{\partial x_j} = \frac{1}{\varepsilon}\partial_{\xi_j}\mathcal{N}(\xi;\eta).$$

Using the explicit representation of the Neumann function (4.1) we get the following value of the derivatives ($j = 1, 2$):

$$\begin{aligned}\partial_{x_j}\mathcal{N}(\xi;\eta) = -\frac{1}{2\pi\varepsilon}\frac{\xi_j - \eta_j}{(\xi_1-\eta_1)^2 + (\xi_2-\eta_2)^2} + \frac{1}{2\pi\varepsilon}\frac{\xi_j}{\xi_1^2+\xi_2^2}\\ - \frac{1}{2\pi\varepsilon}\left[\frac{\xi_j(\eta_1^2+\eta_2^2) - \eta_j}{(\xi_1^2+\xi_2^2-1)(\eta_1^2+\eta_2^2-1) + (\xi_1-\eta_1)^2 + (\xi_2-\eta_2)^2}\right].\end{aligned} \tag{4.10}$$

Now substitute $\xi_j = (1/\varepsilon)(w_j(s,t) - z_{0,j}(t))$, $\eta_j = -(1/\varepsilon)z_{0,j}(t)$, $j = 1, 2$ (in order to simplify the representation we omit the internal variables s and t on the right-hand side of this relation) and calculate the derivatives of two terms of the Maz'ya–Movchan asymptotic formula (see (3.1)) at $\mathbf{x} = (w_1, w_2)$ with $\mathbf{y} = (0,0)$,

$$\frac{\partial}{\partial x_j}\left(\mathcal{N}(\xi,\eta) + \frac{1}{4\pi}\log\left|\frac{1}{\varepsilon}(\mathbf{x}-\mathbf{y})\right|^2\right).$$

These derivatives (denoted K_j) are equal to

$$\begin{aligned}K_j = \frac{\partial}{\partial x_j}\left(\mathcal{N}(\xi,\eta) + \frac{1}{4\pi}\log\left|\frac{1}{\varepsilon}(\mathbf{x}-\mathbf{y})\right|^2\right)\\ = -\frac{1}{2\pi}\left\{\frac{(w_j - z_{0,j})[z_{0,1}^2 + z_{0,2}^2 - \varepsilon^2] + \varepsilon^2 w_j}{[(w_1-z_{0,1})^2 + (w_2-z_{0,2})^2 - \varepsilon^2][z_{0,1}^2 + z_{0,2}^2 - \varepsilon^2] + \varepsilon^2(w_1^2+w_2^2)}\right.\\ \left. - \frac{w_j - z_{0,j}}{(w_1-z_{0,1})^2 + (w_2-z_{0,2})^2}\right\}.\end{aligned} \tag{4.11}$$

Thus for $\varepsilon = 0$, we have $K_j = 0$.

https://doi.org/10.1112/S0025579314000461 Published online by Cambridge University Press

For the regular part $H(\mathbf{x};\mathbf{y})$ of Green's function $G(\mathbf{x};\mathbf{y})$ we have the representation (3.2), i.e.

$$H(\mathbf{x};\mathbf{y}) = \frac{1}{2\pi}\log\left|\frac{g(\mathbf{x};\mathbf{y})}{\mathbf{x}-\mathbf{y}}\right|.$$

Therefore

$$\begin{aligned}
&\partial_{x_j} H(\mathbf{w};O)\\
&= +\frac{1}{2\pi}\frac{g_1(\mathbf{z}_0;O)\partial_{z_{0,j}} g_1(\mathbf{z}_0;O) + g_2(\mathbf{z}_0;O)\partial_{z_{0,j}} g_2(\mathbf{z}_0;O)}{g_1^2(\mathbf{z}_0;O) + g_2^2(\mathbf{z}_0;))} - \frac{1}{2\pi}\frac{z_{0,j}}{z_{0,1}^2 + z_{0,2}^2}\\
&= \frac{1}{2\pi}\left(g_1(\mathbf{w};O)\partial_{w_j} g_1(\mathbf{w};O) + g_2(\mathbf{w};O)\partial_{w_j} g_2(\mathbf{w};O) - \frac{w_j}{w_1^2+w_2^2}\right). \quad (4.12)
\end{aligned}$$

Analogously,

$$\begin{aligned}
\partial_{y_j} H(\mathbf{x};\mathbf{z}_0) = &+\frac{1}{2\pi}\frac{g_1(\mathbf{x};\mathbf{z}_0)\partial_{y_j} g_1(\mathbf{x};\mathbf{z}_0) + g_2(\mathbf{x};\mathbf{z}_0)\partial_{y_j} g_2(\mathbf{x};\mathbf{z}_0)}{g_1^2(\mathbf{x};\mathbf{z}_0) + g_2^2(\mathbf{x};\mathbf{z}_0)}\\
&+\frac{1}{2\pi}\frac{x_j - z_{0,j}}{(x_1-z_{0,1})^2 + (x_2-z_{0,2})^2}. \quad (4.13)
\end{aligned}$$

In this case the right-hand side of the last relation does depend on $\mathbf{x}$.

Now we have to calculate the derivatives with respect to $\mathbf{x}$ of the following expression:

$$\begin{aligned}
J_1(\mathbf{x},\mathbf{y}) := J_1 &= \varepsilon\mathcal{D}\left(\frac{1}{\varepsilon}(\mathbf{x}-\mathbf{z}_0)\right)\cdot\nabla_{\mathbf{x}} H(\mathbf{z}_0;\mathbf{y})\\
&= \varepsilon\mathcal{D}_1\left(\frac{1}{\varepsilon}(\mathbf{x}-\mathbf{z}_0)\right)\partial_{x_1} H(\mathbf{z}_0;\mathbf{y}) + \varepsilon\mathcal{D}_2\left(\frac{1}{\varepsilon}(\mathbf{x}-\mathbf{z}_0)\right)\partial_{x_2} H(\mathbf{z}_0;\mathbf{y}),
\end{aligned}$$

where only first multiplier in each summand depends on $\mathbf{x}$. The derivatives of $\mathcal{D}_k$ in x_j are connected with that in ξ_j:

$$\partial_{x_j}\left(\varepsilon\mathcal{D}_k\left(\frac{1}{\varepsilon}(\mathbf{x}-\mathbf{z}_0)\right)\right) = (\mathcal{D}_k)'_{\xi_j}\left(\frac{1}{\varepsilon}(\mathbf{x}-\mathbf{z}_0)\right), \quad j,k = 1,2.$$

By direct calculation, we have

$$\begin{aligned}
\partial_{x_1} J_1(\mathbf{w},O) = \frac{\varepsilon^2}{2}\Bigg(&\frac{(w_2-z_{0,2})^2 - (w_1-z_{0,1})^2}{((w_1-z_{0,1})^2 + (w_2-z_{0,2})^2)^2}\cdot\partial_{x_1} H(\mathbf{z}_0;O)\\
&-\frac{2(w_1-z_{0,1})(w_2-z_{0,2})}{((w_1-z_{0,1})^2 + (w_2-z_{0,2})^2)^2}\cdot\partial_{x_2} H(\mathbf{z}_0;O)\Bigg) \quad (4.14)
\end{aligned}$$

and

$$\begin{aligned}
\partial_{x_2} J_1(\mathbf{w},O) = \frac{\varepsilon^2}{2}\Bigg(&-\frac{2(w_1-z_{0,1})(w_2-z_{0,2})}{((w_1-z_{0,1})^2 + (w_2-z_{0,2})^2)^2}\cdot\partial_{x_1} H(\mathbf{z}_0;O)\\
&-\frac{(w_2-z_{0,2})^2 - (w_1-z_{0,1})^2}{((w_1-z_{0,1})^2 + (w_2-z_{0,2})^2)^2}\cdot\partial_{x_2} H(\mathbf{z}_0;O)\Bigg), \quad (4.15)
\end{aligned}$$

where the derivatives $\partial_{x_j} H(\mathbf{z}_0;\mathbf{y})$ are presented in (4.12).

https://doi.org/10.1112/S0025579314000461 Published online by Cambridge University Press

Finally, we have

$$J_2(\mathbf{x}, \mathbf{y}) = J_2 = \varepsilon \mathcal{D}\left(\frac{1}{\varepsilon}(\mathbf{y} - \mathbf{z}_0)\right) \cdot \nabla_{\mathbf{y}} H(\mathbf{x}; \mathbf{z}_0)$$
$$= \varepsilon \mathcal{D}_1\left(\frac{1}{\varepsilon}(\mathbf{y} - \mathbf{z}_0)\right) F_1(\mathbf{x}; \mathbf{z}_0) + \varepsilon \mathcal{D}_2\left(\frac{1}{\varepsilon}(\mathbf{y} - \mathbf{z}_0)\right) F_2(\mathbf{x}; \mathbf{z}_0).$$

Here, only the second multiplier in each summand depends on $\mathbf{x}$, and

$$F_i = \partial_{y_i} H(\mathbf{x}; \mathbf{z}_0) = \frac{1}{2\pi} \partial_{y_i} \log \left| \frac{g(\mathbf{x}; \mathbf{y})}{\mathbf{x} - \mathbf{y}} \right|_{\mathbf{y}=\mathbf{z}_0}, \quad i = 1, 2.$$

Hence

$$\partial_{x_j} J_2 = \frac{\varepsilon}{2} \frac{\eta_1}{\eta_1^2 + \eta_2^2} \partial_{x_j} F_1 + \frac{\varepsilon}{2} \frac{\eta_2}{\eta_1^2 + \eta_2^2} \partial_{x_j} F_2, \quad j = 1, 2.$$

Therefore, since $\eta_i = -(1/\varepsilon) z_{0,i}$, $i = 1, 2$, and using (4.6) we have

$$\partial_{x_j} J_2(\mathbf{w}, O) = -\frac{\varepsilon^2}{2} \frac{z_{0,1}}{z_{0,1}^2 + z_{0,1}^2} \cdot \partial_{x_j} F_1(\mathbf{w}; \mathbf{z}_0) - \frac{\varepsilon^2}{2} \frac{z_{0,2}}{z_{0,1}^2 + z_{0,1}^2} \cdot \partial_{x_j} F_2(\mathbf{w}; \mathbf{z}_0). \tag{4.16}$$

4.3. *Integrals of Green's function.* In this subsection we calculate integrals from the right-hand side of equation (vi) in the representation of Problem ($\mathrm{HS}_{\mathrm{move}}$):

$$P_j = \frac{Q\varepsilon}{m} \int_0^{2\pi} \mathcal{G}(\mathbf{x}; \mathbf{y}; t) n_j^{(\mathrm{in})}(\theta)\, d\theta, \quad j = 1, 2, \tag{4.17}$$

were $\mathbf{x} = (z_{0,1} + \varepsilon \cos\theta, z_{0,2} + \varepsilon \sin\theta)$, $\mathbf{y} = (0, 0)$.

In our calculations we use components of formula (3.1) and their representations obtained in §4.1. First we calculate the integral

$$I_{1,1} := \int_0^{2\pi} G(\mathbf{x}; \mathbf{y}; t) \cos\theta\, d\theta \Big|_{\mathbf{y}=O} \tag{4.18}$$

employing representation (4.3):

$$I_{1,1} = -\frac{1}{2\pi} \int_0^{2\pi} \log |g(\mathbf{x}; O)| \cos\theta\, d\theta = -\frac{1}{2\pi} \mathrm{Re} \int_0^{2\pi} \log g(\mathbf{x}; O) \cos\theta\, d\theta.$$

Note that for each fixed $t \in I$ the function $\log g(\mathbf{x}; O)$ is analytic with respect to the variable $\mathbf{x} = (x_1, x_2)$ in the disc $B(\mathbf{z}_0, \varepsilon)$. Hence using the Taylor expansion of $\log g(\mathbf{x}; O)$ at $\mathbf{x} = \mathbf{z}_0$, we have

$$I_{1,1} = -\frac{\varepsilon}{2} \mathrm{Re}\, c_1 + O(\varepsilon^3) = -\frac{\varepsilon}{2} \mathrm{Re}\, \frac{g'(\mathbf{z}_0, O)}{g(\mathbf{z}_0, O)} + O(\varepsilon^3). \tag{4.19}$$

https://doi.org/10.1112/S0025579314000461 Published online by Cambridge University Press

Similar calculations can be performed for the integral

$$\tilde{I}_{1,1} := \int_0^{2\pi} G(\mathbf{x};\mathbf{y};t)\sin\theta\,d\theta\Big|_{\mathbf{y}=O} = -\frac{\varepsilon}{2}\operatorname{Re} \mathrm{i}c_1 + O(\varepsilon^3)$$
$$= -\frac{\varepsilon}{2}\operatorname{Re}\frac{\mathrm{i}g'(\mathbf{z}_0,O)}{g(\mathbf{z}_0,O)} + O(\varepsilon^3). \quad (4.20)$$

In the integral

$$I_{1,2} := \int_0^{2\pi}\left[\mathcal{N}\left(\frac{1}{\varepsilon}(\mathbf{x}-\mathbf{z}_0,\mathbf{y}-\mathbf{z}_0)\right)+\frac{1}{2\pi}\log\left|\frac{1}{\varepsilon}(\mathbf{x}-\mathbf{y})\right|\right]\cos\theta\,d\theta\Big|_{\mathbf{y}=O}, \quad (4.21)$$

we use representation (4.1):

$$I_{1,2} := \int_0^{2\pi}\left[\mathcal{N}\left(\frac{1}{\varepsilon}(\mathbf{x}-\mathbf{z}_0,-\mathbf{z}_0)\right)+\frac{1}{2\pi}\log\left|\frac{\mathbf{x}}{\varepsilon}\right|\right]\cos\theta\,d\theta$$
$$= -\frac{1}{4\pi}\int_0^{2\pi}\log\left\{\left(\frac{|\mathbf{x}-\mathbf{z}_0|^2}{\varepsilon^2}-1\right)\left(\frac{|\mathbf{z}_0|^2}{\varepsilon^2}-1\right)+\frac{|\mathbf{x}|^2}{\varepsilon^2}\right\}\cos\theta\,d\theta$$
$$+\frac{1}{4\pi}\int_0^{2\pi}\log\left(\frac{|\mathbf{x}-\mathbf{z}_0|^2|\mathbf{z}_0|^2}{\varepsilon^4}\right)\cos\theta\,d\theta. \quad (4.22)$$

Since $|\mathbf{x}-\mathbf{z}_0|=\varepsilon$ and $\int_0^{2\pi} C\cdot\cos\theta\,d\theta = 0$, we have

$$I_{1,2} = -\frac{1}{2\pi}\int_0^{2\pi}\log|\mathbf{x}|\cos\theta\,d\theta = -\frac{1}{2\pi}\operatorname{Re}\int_0^{2\pi}\log\mathbf{x}\cos\theta\,d\theta.$$

The function $\log\mathbf{x}$ is an analytic function with respect to the variable $\mathbf{x}=(x_1, x_2)$ in the disc $B(\mathbf{z}_0,\varepsilon)$. Hence

$$I_{1,2} = -\frac{\varepsilon}{2}\operatorname{Re}\frac{1}{\mathbf{z}_0} + O(\varepsilon^3). \quad (4.23)$$

Analogously, for the integral $\tilde{I}_{1,2}$ we have

$$\tilde{I}_{1,2} := \int_0^{2\pi}\left[\mathcal{N}\left(\frac{1}{\varepsilon}(\mathbf{x}-\mathbf{z}_0,\mathbf{y}-\mathbf{z}_0)\right)+\frac{1}{2\pi}\log\left|\frac{1}{\varepsilon}(\mathbf{x}-\mathbf{y})\right|\right]\sin\theta\,d\theta\Big|_{\mathbf{y}=O}$$
$$= -\frac{1}{2\pi}\int_0^{2\pi}\log|\mathbf{x}|\sin\theta\,d\theta$$
$$= -\frac{1}{2\pi}\operatorname{Re}\int_0^{2\pi}\log\mathbf{x}\sin\theta\,d\theta = -\frac{\varepsilon}{2}\operatorname{Re}\frac{\mathrm{i}}{\mathbf{z}_0} + O(\varepsilon^3). \quad (4.24)$$

Next we calculate

$$I_{1,3} := \int_0^{2\pi}\varepsilon\mathcal{D}\left(\frac{1}{\varepsilon}(\mathbf{x}-\mathbf{z}_0)\right)\cdot\nabla_{\mathbf{x}}H(\mathbf{z}_0;\mathbf{y})\cos\theta\,d\theta. \quad (4.25)$$

https://doi.org/10.1112/S0025579314000461 Published online by Cambridge University Press

Taking into account exact values (4.6) of the functions $\mathcal{D}_1(\xi)$, $\mathcal{D}_2(\xi)$ and parametrization of the boundary of $B(0;1)$ ($\xi_1=\cos\theta$, $\xi_2=\sin\theta$), we obtain

$$\begin{aligned} I_{1,3} &= \frac{\varepsilon}{2}\partial_{x_1}H(\mathbf{z}_0;\mathbf{y})\int_0^{2\pi}\cos^2\theta\,d\theta+\frac{\varepsilon}{2}\partial_{x_2}H(\mathbf{z}_0;\mathbf{y})\int_0^{2\pi}\sin\theta\cos\theta\,d\theta \\ &= \frac{\pi\varepsilon}{2}\partial_{x_1}H(\mathbf{z}_0;\mathbf{y}). \end{aligned}$$

Finally, using (4.12),

$$I_{1,3}=\frac{\varepsilon}{4}\left(\frac{g_1(\mathbf{z}_0;O)\partial_{x_1}g_1(\mathbf{z}_0;O)+g_2(\mathbf{z}_0;O)\partial_{x_1}g_2(\mathbf{z}_0;O)}{g_1^2(\mathbf{z}_0;O)+g_2^2(\mathbf{z}_0;O)}-\frac{z_{0,1}}{z_{0,1}^2+z_{0,2}^2}\right). \tag{4.26}$$

Similar calculations lead to

$$\begin{aligned} \tilde{I}_{1,3} &:= \int_0^{2\pi}\varepsilon\mathcal{D}\left(\frac{1}{\varepsilon}(\mathbf{x}-\mathbf{z}_0)\right)\cdot\nabla_{\mathbf{x}}H(\mathbf{z}_0;\mathbf{y})\sin\theta\,d\theta=\frac{\pi\varepsilon}{2}\partial_{x_2}H(\mathbf{z}_0;\mathbf{y}) \\ &= \frac{\varepsilon}{4}\left(\frac{g_1(\mathbf{z}_0;O)\partial_{x_2}g_1(\mathbf{z}_0;O)+g_2(\mathbf{z}_0;O)\partial_{x_2}g_2(\mathbf{z}_0;O)}{g_1^2(\mathbf{z}_0;O)+g_2^2(\mathbf{z}_0;O)}-\frac{z_{0,2}}{z_{0,1}^2+z_{0,2}^2}\right). \end{aligned} \tag{4.27}$$

The last integral from (4.17) is calculated by using (4.6):

$$\begin{aligned} I_{1,4} &:= \int_0^{2\pi}\varepsilon\mathcal{D}\left(\frac{1}{\varepsilon}(\mathbf{y}-\mathbf{z}_0)\right)\cdot\nabla_{\mathbf{y}}H(\mathbf{x};\mathbf{z}_0)\cos\theta\,d\theta \\ &= -\frac{\varepsilon^2}{2(z_{0,1}^2+z_{0,2}^2)}\int_0^{2\pi}[z_{0,1}\partial_{y_1}H(\mathbf{x};\mathbf{z}_0)+z_{0,2}\partial_{y_2}H(\mathbf{x};\mathbf{z}_0)]\cos\theta\,d\theta. \end{aligned} \tag{4.28}$$

Since $\log\left(g(\mathbf{x};\mathbf{z}_0)/(\mathbf{x}-\mathbf{z}_0)\right)$ is an analytic function with respect to the variable $\mathbf{x}=(x_1,x_2)$ in the disc $B(\mathbf{z}_0,\varepsilon)$,

$$-\frac{Q\varepsilon}{m}I_{1,4}=O(\varepsilon^4).$$

Similarly, we obtain

$$\begin{aligned} \tilde{I}_{1,4} &:= \int_0^{2\pi}\varepsilon\mathcal{D}\left(\frac{1}{\varepsilon}(\mathbf{y}-\mathbf{z}_0)\right)\cdot\nabla_{\mathbf{y}}H(\mathbf{x};\mathbf{z}_0)\sin\theta\,d\theta, \\ -\frac{Q\varepsilon}{m}\tilde{I}_{1,4} &= O(\varepsilon^4). \end{aligned} \tag{4.29}$$

Note that

$$\begin{aligned} \operatorname{Re}\frac{g'(\mathbf{z}_0,O)}{g(\mathbf{z}_0,O)} &= \frac{g_1(\mathbf{z}_0;O)\partial_{x_1}g_1(\mathbf{z}_0;O)+g_2(\mathbf{z}_0;O)\partial_{x_1}g_2(\mathbf{z}_0;O)}{g_1^2(\mathbf{z}_0;O)+g_2^2(\mathbf{z}_0;O)}, \\ \operatorname{Re}\mathrm{i}\frac{g'(\mathbf{z}_0,O)}{g(\mathbf{z}_0,O)} &= \frac{g_1(\mathbf{z}_0;O)\partial_{x_2}g_1(\mathbf{z}_0;O)+g_2(\mathbf{z}_0;O)\partial_{x_2}g_2(\mathbf{z}_0;O)}{g_1^2(\mathbf{z}_0;O)+g_2^2(\mathbf{z}_0;O)}, \end{aligned}$$

https://doi.org/10.1112/S0025579314000461 Published online by Cambridge University Press

$$\operatorname{Re}\frac{1}{\mathbf{z}_0}=\frac{z_{0,1}}{z_{0,1}^2+z_{0,2}^2},\qquad \operatorname{Re}\frac{\mathrm{i}}{\mathbf{z}_0}=\frac{z_{0,2}}{z_{0,1}^2+z_{0,2}^2}.$$

Combining all the above calculations, we have

$$-\frac{Q\varepsilon}{m}[I_{1,1}+I_{1,2}+I_{1,3}+I_{1,4}]=\frac{Q\varepsilon^2}{4m}I+O(\varepsilon^4), \tag{4.30}$$

$$-\frac{Q\varepsilon}{m}[\tilde{I}_{1,1}+\tilde{I}_{1,2}+\tilde{I}_{1,3}+\tilde{I}_{1,4}]=\frac{Q\varepsilon^2}{4m}\tilde{I}+O(\varepsilon^4), \tag{4.31}$$

$$I=\frac{g_1(\mathbf{z}_0;\,O)\partial_{x_1}g_1(\mathbf{z}_0;\,O)+g_2(\mathbf{z}_0;\,O)\partial_{x_1}g_2(\mathbf{z}_0;\,O)}{g_1^2(\mathbf{z}_0;\,O)+g_2^2(\mathbf{z}_0;\,O)}+3\frac{z_{0,1}}{z_{0,1}^2+z_{0,2}^2},$$

$$\tilde{I}=\frac{g_1(\mathbf{z}_0;\,O)\partial_{x_2}g_1(\mathbf{z}_0;\,O)+g_2(\mathbf{z}_0;\,O)\partial_{x_2}g_2(\mathbf{z}_0;\,O)}{g_1^2(\mathbf{z}_0;\,O)+g_2^2(\mathbf{z}_0;\,O)}+3\frac{z_{0,2}}{z_{0,1}^2+z_{0,2}^2}.$$

4.4. *Final system of differential equations.* It follows from the potential theory (see, for example [**9**, Ch. 8]; cf. [**18**, Lemma 2.3]) that for any compact subset $\Omega,\overline{\Omega}\subset D_1(t)$,

$$|(r_\varepsilon(\mathbf{x},\mathbf{y}))'_{x_j}|\leqslant\varepsilon^3,\quad j=1,2,\ \mathbf{x},\mathbf{y}\in\overline{\Omega}.$$

Thus, Problem ($\mathrm{HS}_{\mathrm{move}}$) can be asymptotically approximated by the following system:

$$\partial_t w_1=-\frac{Qh^2}{12\mu}(\partial_{x_1}G(\mathbf{w};\,O)+K_1+\partial_{x_1}J_1(\mathbf{w};\,O)+\partial_{x_1}J_2(\mathbf{w};\,O)), \tag{4.32}$$

$$\partial_t w_2=-\frac{Qh^2}{12\mu}(\partial_{x_2}G(\mathbf{w};\,O)+K_2+\partial_{x_2}J_1(\mathbf{w};\,O)+\partial_{x_2}J_2(\mathbf{w};\,O)), \tag{4.33}$$

$$z''_{0,1}+\frac{\kappa\pi\varepsilon^2}{m}z'_{0,1}=\frac{Q\varepsilon^2}{4m}I, \tag{4.34}$$

$$z''_{0,2}+\frac{\kappa\pi\varepsilon^2}{m}z'_{0,2}=\frac{Q\varepsilon^2}{4m}\tilde{I}, \tag{4.35}$$

with initial conditions $\mathbf{z}_0(0)=\mathbf{z}^{(0)}$, $\mathbf{z}'_0(0)=\mathbf{z}^{(1)}$. Here $\mathbf{w}=(w_1(s,t),w_2(s,t))$ is an unknown parametrization of the external boundary $\partial D(t)$, $\mathbf{z}_0=(z_{0,1}(t),z_{0,2}(t))$ is an unknown position of the center of the moving obstacle and K_j, $\partial_{x_j}J_k$, I, $\tilde{I}$ are defined in (4.11), (4.14)–(4.16), (4.30), (4.31).

§5. *Numerical examples and discussions.* In this section we provide only a short illustration of the efficiency of the proposed methods for applications.

The numerical scheme to obtain the solution employs reduction of the system of governing equations (4.32)–(4.33) to the system of ODEs of first order, where the velocity of the inclusion is introduced as an additional dependent variable. In order to solve the first-order dynamic system derived in this way we utilize the standard ODE solver from the Matlab package: ode45. It is based

https://doi.org/10.1112/S0025579314000461 Published online by Cambridge University Press

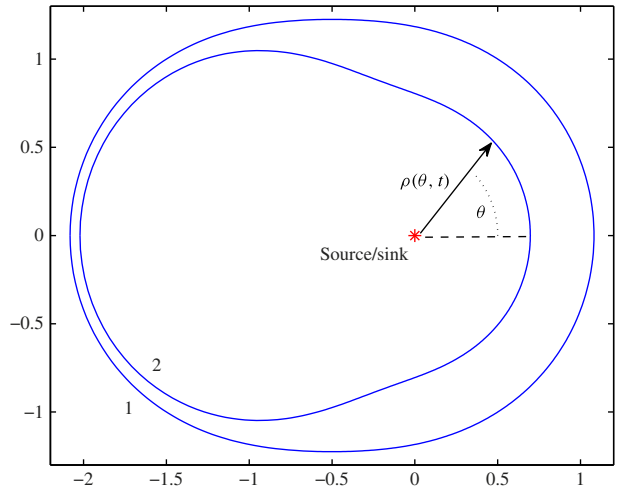


Figure 1: Evolution of the computational domain in time—the limiting curves. The vector $\rho(\theta, t)$ defines the boundary curve.

on an explicit Runge–Kutta formula. The respective conformal mappings of the boundary curve are performed by means of the Schwartz–Christoffel toolbox [**4**, **5**]. The derivatives of the mapping along the free boundary are computed by our own subroutines, based on a spline approximation.

To investigate the accuracy of the proposed numerical scheme we use the classical benchmark by Polubarinova-Kochina [**12**, p. 29], which describes the fluid domain induced by a source or a sink without inclusion ($\varepsilon = 0$). The evolution of the free boundary in the case considered is illustrated in Figure 1. We analyze three different densities of the spatial meshing, described by the number of nodes, N, distributed at uniform angular distances: $N = 35$, $N = 70$, $N = 140$. Moreover, both the fluid source and fluid sink variants are considered. In the first case the free boundary evolves from the internal to the external shape (see Figure 1). In the second one it moves in reverse direction. The results of computations illustrated by the relative error of the radius vector defining the free boundary, $\delta\rho$, are shown in Figures 2–3.

As can be seen in the figures, in the range of N analyzed, a doubling of the number of points reduces the computation error by an order of magnitude. What is more, the solution accuracy depends essentially on the variant of domain evolution. Better results (up to one order of magnitude) are observed for the domain expansion (fluid source). Especially pronounced differences are manifested at the angular distances at which the shape deformation is biggest ($\theta \leqslant \pm\pi/2$). A distribution of $\delta\rho$ symmetrical with respect to $\theta = 0$ is a consequence of the problem symmetry, and additionally confirms the quality of our results. It is also worth mentioning that in the variants under investigation, doubling the number of points N leadings to a doubling of the computation time.

https://doi.org/10.1112/S0025579314000461 Published online by Cambridge University Press

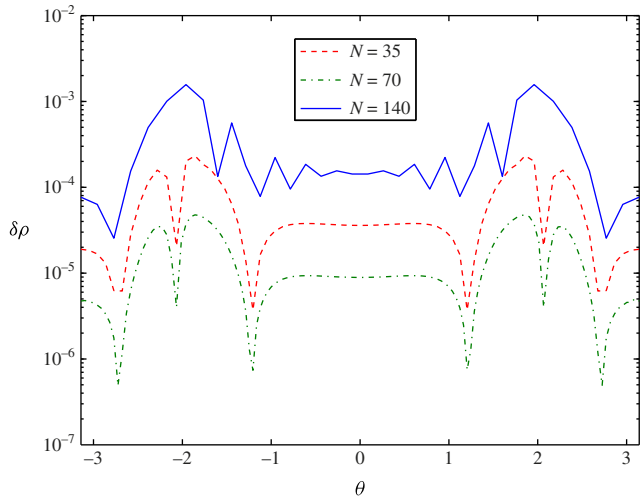


Figure 2: The relative error of the radius vector, $\delta\rho$, for the domain expansion (fluid source).

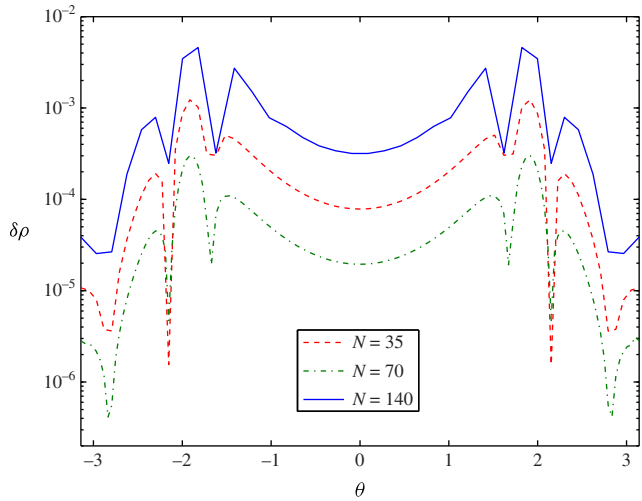


Figure 3: The relative error of the radius vector, $\delta\rho$, for the domain contraction (fluid sink).

In the following numerical examples we decided to use $N = 70$. According to the tests presented above, this should guarantee solution accuracy of the order of at least 10^{-4}.

In the next step we investigate to what degree the presence of an immobile inclusion inside the domain affects the fluid flow. We restrict ourselves to the fluid source case and consider a circular inclusion of radius $\varepsilon = 0.2$ encircled by the internal curve 2 from the previous benchmark. We retain the same source intensity and time interval. Two locations of the inclusion are considered: $\mathbf{z}_0 = 0.2 + 0.5\mathrm{i}$ and $\mathbf{z}_0 = -1.55 - 0.55\mathrm{i}$. Figure 4 provides a graphical illustration of

https://doi.org/10.1112/S0025579314000461 Published online by Cambridge University Press

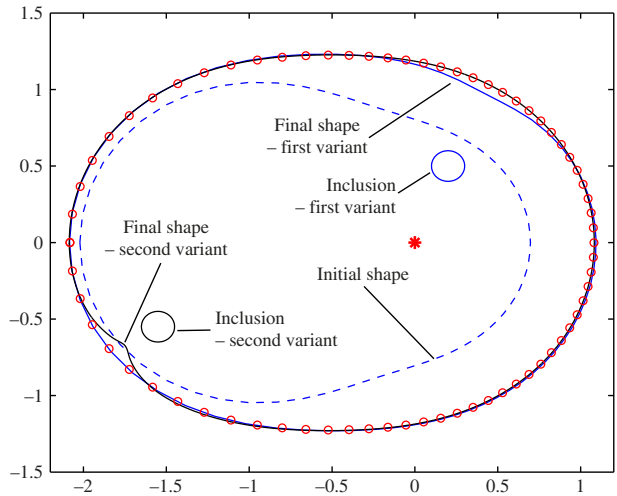


Figure 4: (Colour online) Graphical illustration of the problem with an immobile inclusion. Two locations of the obstacle are considered. The curve with markers corresponds to the results for undisturbed flow (without inclusion).

the problem, where the final shapes for the free boundary for both variants are compared with the case of undisturbed flow depicted with markers.

Since in both cases the source supplies the same volume of fluid in the time considered, one can independently check the accuracy of computations in terms of the fluid balance. The relative deviations of the fluid volume from the benchmark value were 1.64×10^{-6} and 4.51×10^{-5} for the first and second location of the obstacle, respectively. We believe that the second value is greater due to the integration error itself, as the relative deviation of ρ has a much sharper maximum in this case. However, both results suggest very good solution accuracy as well as very good quality of the Green function approximation, even for relatively large magnitude of the small parameter ε. Note that accuracy of the uniform asymptotic formula increases (decreases) with time in the source (sink) case.

Next, we consider the inclusion with two degrees of freedom (translations) analyzing its movement in two cases. In the first case, the friction term in equations (4.34)–(4.35) is neglected. The second variant accounts for the friction phenomenon. In both cases we assume that initial position of the inclusion is $\mathbf{z}_0(0) = 0.1 + 0.1\mathrm{i}$ and its initial velocity is zero.

Figure 5 shows the evolution of the free boundary and the obstacle movement. Starting from zero initial velocity, the obstacle moves rectilinearly along the line: the straight line containing the source and the center of the corresponding inclusion. Although in the case analyzed the obstacle translations are quite different from each other, the free boundary shapes for both variants are almost identical. The balance condition is satisfied this time to the level of 10^{-8}.

In the last part of our analysis we consider the problem when the initial velocity of the inclusion has a non-zero value, and its vector is not collinear

https://doi.org/10.1112/S0025579314000461 Published online by Cambridge University Press

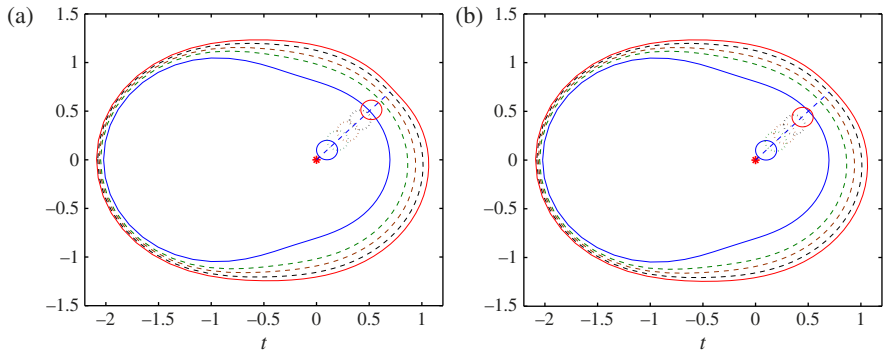


Figure 5: (Colour online) The domain evolution and obstacle movement for: (a) the frictionless case; (b) the variant with friction. Dashed lines illustrate selected intermediate positions.

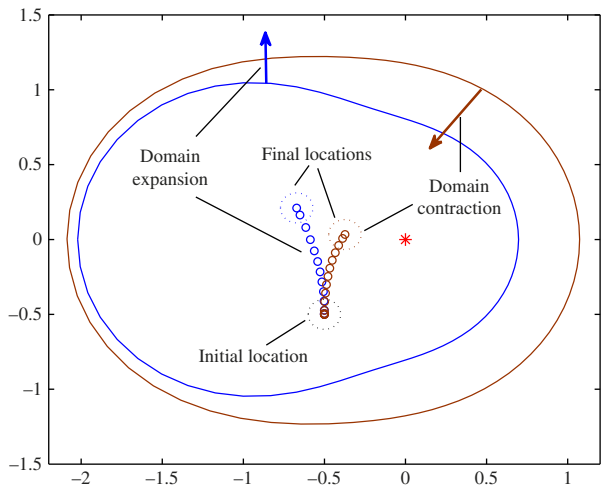


Figure 6: (Colour online) Domain configuration and obstacle movement. Markers correspond to intermediate positions of the inclusion. The depicted boundary curves define the initial shapes of the domain for respective variants of the problem.

with the line: the straight line containing the source and the center of the corresponding inclusion. It is assumed that the initial position of the obstacle is $\mathbf{z}_0(0) = -0.5 - 0.5\mathrm{i}$, while its initial velocity yields $\mathbf{v}(0) = 2\mathrm{i}$. We consider two variants, depicted in Figure 6. In the first, the fluid flow is driven by the source, and the initial shape of the free boundary is described by the internal curve. The second variant assumes the domain contraction caused by the fluid sink. Here, the initial domain is defined by the external curve. The fluid balance equation was satisfied to the level of 10^{-8} for the variant of domain expansion, and 10^{-7} for domain contraction. The traces of inclusion for both cases are shown by markers.

It should be emphasized that the initial conditions imposed do not imply kinematic equivalence between both variants of the problem. The curvatures

https://doi.org/10.1112/S0025579314000461 Published online by Cambridge University Press

of the tracks (bend directions) and the signs of respective components of acceleration are determined by the source/sink activity. In the case of domain expansion the fluid flow direction magnifies the obstacle velocity. Thus the distance covered is greater than that for the fluid sink. Obviously, for other configurations of the initial velocity vector one can expect different trends.

Concluding this section, we have shown that the method utilizing the uniform asymptotic expansion for the Green function delivered in [**18**] is effective and the computations based on that approach are stable and robust.

Acknowledgements. The work by G.M. and S.R. has been supported by PEOPLE IAPP Project PIAP-GA-2009-251475 HYDROFRAC and by PEOPLE IAPP Project IAPP-GA-284544 PARM2. The work by M.W. has been supported by PIAP-GA-2011-286110 INTERCER2. The authors are thankful to Dr. M. Nives for fruitful discussion of the problem that forms the subject of this paper.

References

1. S. N. Antontsev, C. R. Gonçalves and A. M. Meirmanov, Local existence of classical solutions to the well-posed Hele-Shaw problem. *Port. Math. (N.S.)* **59**(4) (2002), 435–452.
2. S. N. Antontsev, C. R. Gonçalves and A. M. Meirmanov, Exact estimates for the classical solutions to the free-boundary problem in the Hele-Shaw cell. *Adv. Differ. Equ.* **8**(10) (2003), 1259–1280.
3. M. C. Dallaston and S. W. McCue, New exact solutions for Hele-Shaw flow in doubly connected regions. *Phys. Fluids* **24** (2012), 052101.
4. T. A. Driscoll, Algorithm 756: A MATLAB toolbox for Schwarz–Christoffel mapping. *ACM Trans. Math. Software* **22** (1996), 168–186.
5. T. A. Driscoll, Algorithm 843: Improvements to the Schwarz–Christoffel toolbox for MATLAB. *ACM Trans. Math. Software* **31** (2005), 239–251.
6. V. Entov and P. Etingof, On the break of air bubbles in a Hele-Shaw cell. *European J. Appl. Math.* **22**(2) (2011), 125–149.
7. J. Escher and G. Simonett, Classical solutions of multidimensional Hele-Shaw models. *SIAM J. Math. Anal.* **28**(5) (1997), 1028–1047.
8. L. A. Galin, Unsteady filtration with a free surface. *Dokl. Akad. Nauk USSR* **47** (1945), 246–249 (in Russian).
9. D. Gilbarg and N. S. Trudinger, *Elliptic Partial Differential Equations of Second Order*, 2nd edn., Springer (Berlin, 2001).
10. I. S. Gradshteyn and I. M. Ryzhik, *Table of Integrals, Series, and Products*, 7th edn., Elsevier (Amsterdam, 2007).
11. B. Gustafsson, On a differential equation arising in a Hele-Shaw flow moving boundary problem. *Ark. Mat.* **22** (1984), 251–268.
12. B. Gustafsson and A. Vasil'ev, *Conformal and Potential Analysis in Hele-Shaw Cells*, Birkhäuser Verlag (Basel, 2006).
13. J. Hadamard, Sur le problème d'analyse relatif à l'equilibre des plaques élastiques encastrées. In *Memoire Couronne en 1907 par l'Academie: Prix Vaillant, Mémoires Présentés par Divers Savants à lÁcademie des Sciences, Vol. 33, No. 4, 1908* (*Oeuvres de Jasques Hadamard* **2**), Centre National de la Recherche Scientifique (Paris, 1968), 515–629.
14. H. S. Hele-Shaw, The flow of water. *Nature* **58**(1489) (1898), 33–36.
15. Yu. E. Hohlov and M. Reissig, On classical solvability for the Hele-Shaw moving boundary problem with kinetic undercooling regularization. *European J. Appl. Math.* **6** (1995), 421–439.
16. V. Maz'ya and A. Movchan, Uniform asymptotics of Green's kernels for mixed and Neumann problems in domains with small holes and inclusions. In *Sobolev Spaces in Mathematics. III: Applications in Mathematical Physics* (*International Mathematical Series* **10**) (ed. V. Isakov), Springer and Tamara Rozhkovskaya Publisher, Novosibirsk (New York, 2009), 277–316.
17. V. Maz'ya and A. Movchan, Uniform asymptotics of Green's kernels in perforated domains and meso-scale approximation. *Complex Var. Elliptic Equ.* **57**(2) (2012), 137–154.

https://doi.org/10.1112/S0025579314000461 Published online by Cambridge University Press

18. V. Maz'ya, A. Movchan and M. Nieves, *Green's Kernel and Meso-Scale Approximations in Perforated Domains* (*Lecture Notes in Mathematics* **2077**), Springer (Heidelberg, 2013).
19. G. Mishuris, S. Rogosin and M. Wrobel, Hele-Shaw flow with a small obstacle. *Meccanica* **49**(9) (2014), 2037–2047, doi:10.1007/S11012-014-9919-8.
20. G. Mishuris, S. Rogosin and M. Wrobel, Moving stone in the Hele-Shaw flow. *Preprint*, 2014, arXiv:1404.3547v2 [physics.flu-dyn].
21. N. Papamichael, *Lectures on Numerical Conformal Mapping*, University of Cyprus, 2008.
22. P. Ya. Polubarinova-Kochina, On the motion of the oil contour. *Dokl. Akad. Nauk SSSR* **47** (1945), 254–257 (in Russian).
23. M. Reissig, The existence and uniqueness of analytic solutions for moving boundary value problem for Hele-Shaw flows in the plane. *Nonlinear Anal.* **23**(5) (1994), 565–576.
24. A. Vasil'ev, From the Hele-Shaw experiment to integrable systems: a historical overview. *Complex Anal. Oper. Theory* **3** (2009), 551–585.

Gennady Mishuris,
Aberystwyth University,
Penglais,
Aberystwyth SY23 3BZ,
U.K.
E-mail: ggm@aber.ac.uk

Michal Wrobel,
Aberystwyth University,
Penglais,
Aberystwyth SY23 3BZ,
U.K.
E-mail: miw15@aber.ac.uk

Sergei Rogosin,
Aberystwyth University,
Penglais,
Aberystwyth SY23 3BZ,
U.K.
E-mail: ser14@aber.ac.uk
and
Belarusian State University,
Nezavisimosti Ave., 4,
220030 Minsk,
Belarus
E-mail: rogosin@bsu.by

https://doi.org/10.1112/S0025579314000461 Published online by Cambridge University Press